

## Effects of RLC Parameters of a Measuring Circuit on the Frequency Spectrum of Partial Discharges

Castro Heredia, Luis Carlos; Mor, Armando Rodrigo

**DOI**

[10.1109/EIC.2018.8481131](https://doi.org/10.1109/EIC.2018.8481131)

**Publication date**

2018

**Document Version**

Final published version

**Published in**

2018 IEEE Electrical Insulation Conference, EIC 2018

**Citation (APA)**

Castro Heredia, L. C., & Mor, A. R. (2018). Effects of RLC Parameters of a Measuring Circuit on the Frequency Spectrum of Partial Discharges. In *2018 IEEE Electrical Insulation Conference, EIC 2018* (pp. 196-199). Article 8481131 IEEE. <https://doi.org/10.1109/EIC.2018.8481131>

**Important note**

To cite this publication, please use the final published version (if applicable). Please check the document version above.

**Copyright**

Other than for strictly personal use, it is not permitted to download, forward or distribute the text or part of it, without the consent of the author(s) and/or copyright holder(s), unless the work is under an open content license such as Creative Commons.

**Takedown policy**

Please contact us and provide details if you believe this document breaches copyrights. We will remove access to the work immediately and investigate your claim.

# Effects of RLC parameters of a measuring circuit on the frequency spectrum of partial discharges

Luis Carlos Castro Heredia<sup>1</sup>  
Department of Electrical Sustainable Energy  
Delft University of Technology  
Delft, The Netherlands  
L.C.CastroHeredia@tudelft.nl

Armando Rodrigo Mor  
Department of Electrical Sustainable Energy  
Delft University of Technology  
Delft, The Netherlands  
A.RodrigoMor@tudelft.nl

**Abstract**—With the availability of modern acquisition systems it has been possible to measure partial discharge (PD) pulses with enough bandwidth as to record its pulse shape. This new approach has made possible to compute new parameters that were not possible with the tradition narrow band measurements guided by the standard IEC60270. However, broader bandwidth also means more chances to measure noise and disturbances. The measuring circuit plays a main role because it may be the cause of resonances that distort the shape of the PD pulses. This paper presents a test set-up design that contributes to control the RLC parameters of the detection circuit and thus reduce the distortions such as oscillations of the PD pulses. The RLC parameters are estimated by means of a simple but novel procedure where a fast pulse from a calibrator is induced in the detection circuit leading to an easy detection of resonance frequencies.

**Keywords**—partial discharge, frequency response, resonance frequency, ground inductance.

## I. INTRODUCTION

With the availability of modern digital acquisition systems, featuring broad bandwidths from MHz to GHz and sampling rates up to several GS/s, it is nowadays possible to record the shape of partial discharge (PD) pulses. New techniques have exploited the information contained in it for separation [1], classification and recognition of partial discharge sources. This implies much more information than the traditionally obtained by instruments complying with the IEC270 standard but also it comes to a price. For example, the digital acquisition parameters can affect the computation of high frequency parameters as was shown in [2].

The main challenge when attempting to record PD pulse shapes is to overcome the interaction of the pulse with the detection circuit and with the test object itself. At the source of the PD, the pulse is characterized by a wide frequency content as a result of its very short rise time, and if ideally measured, it should be a non-oscillatory signal [3]. However, as the PD pulse cannot be measured in its origin but externally in the terminals of a sensor or a measuring impedance in the detection circuit, it will suffer distortion and attenuation due to the interaction with the measuring system and the sensor. Thus, the PD pulse may be measured as an oscillatory signal

with different amplitude and characteristics than the PD pulse in the origin. These oscillation, as described in [4], lead to increase the error of fundamental PD parameters like charge and energy.

This distortion and attenuation come from the interaction between the PD pulse and the parameters of the detection circuit. Long leads and connection cables usually produce an LC response of the detection circuit, resulting in distortion and attenuation of the PD pulse. With largely inductive test objects such a rotating machines, or long cables, the PD pulses interact also with the transmission line parameters that suppose the test object itself, resulting in an additional source of distortion and attenuation [5,6].

While this source of distortion is unavoidable with largely inductive test objects, in laboratory set-ups for small test samples, this interaction might be controlled and suppressed to some extent.

Therefore, knowing the RLC parameters of the detection circuit helps to find resonance peaks and to tune the circuit to reduce calculation errors in the pulse shape-based parameters. In order to meet these goals, we have developed a methodology for practical estimation of the frequency response of a laboratory test set-up (concentrated parameters) upon the induction of a fast current pulse into the detection circuit. The main circuit frequency response will be explained in terms of the resonance of a series RLC circuit model.

This frequency characterization serves three main purposes. Firstly, it allows to check if oscillations of the pulses are due to avoidable resonances in the detection circuit. Secondly, it allows to estimate and add a damping resistor to reduce resonance peaks. Finally, this methodology can be used to check proper design of measuring systems.

## II. MEASURING SET-UP

The main elements that are needed for partial discharge measurements according to the IEC26070 can be listed as: a blocking inductor ( $Z$ ), a coupling capacitor ( $C_k$ ), a measuring impedance ( $Z_{mi}$ ), a measuring unit (MI) and secondary elements depending on the needs. A common arrangement of such elements is that shown in Fig. 1 [7]. Any PD pulse that is produced in the test object arrives to its terminals and flows through the coupling capacitor and the measuring impedance that form the detection circuit (the high-voltage loop). The output voltage signal from the measuring impedance is then

<sup>1</sup> Also member of Conversion Energy Research Group, Convergía, Universidad del Valle, Colombia.

transmitted to the measuring instrument for processing. It is worth mentioning that this arrangement is valid not only for measurements according to the IEC60270 standard but also for unconventional measurements that use sensors such as high frequency current transformers (HFCT) rather than measuring impedances.

Roughly speaking, the schematic of Fig. 1 corresponds to a capacitive circuit only when the connections between the test object and the coupling capacitor are made very short. In fact, Fig. 1 does not offer the user any indication of the effect and dimensions of the connections, which in practice can be several meters in length.

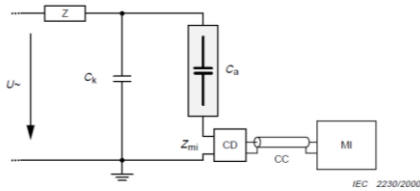


Fig. 1. Schematic of a general PD measuring circuit.

As the connections become larger, an equivalent inductance (also referred as to ground inductance or parasitic inductance) is added to the high-voltage loop, which leads to a LC response of the detection circuit. This inductance acts as a high impedance for the higher frequencies contained in the PD pulse, therefore they get attenuated. This attenuation of the higher frequencies shortens the frequency spectrum of the PD pulse which may account for oscillations.

Moreover, the measurement results might be being inadvertently altered by the length of the connection cables used when testing different samples. Since the objective of this paper is to estimate experimentally the parameters of the detection circuit, then it is necessary to design a set-up that allows strict control of the high-voltage loop length such as that shown in Fig. 2. Detailed specifications of this set-up can be found in [8].

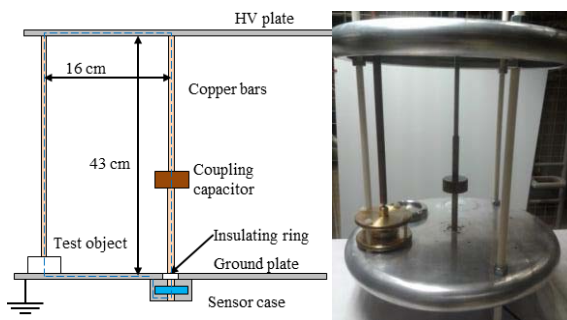


Fig. 2. Concentric and symmetrical test set-up.

The design of Fig. 2 houses the coupling capacitor, the HFCT sensor and the test object in a rigid structure. One of the main features of this design is that the high-voltage and ground electrodes are circular plates with the coupling capacitor in the centre. When the test objects are placed concentrically to the coupling capacitor the same high-voltage loop length is warranted. This concentric, symmetrical and rigid structure helps to keep the same detection circuit for every test object. In

addition its simple design can be reproduced easily by other users contributing to the reproducibility of results.

### III. CIRCUIT INDUCTANCE

The detection circuit illustrated by Fig. 2 has a capacitive component determined by the capacitance of the coupling capacitor and the test object, a resistive component that can be neglected and an inductive component that results from the geometry of the high voltage loop. If the test object is removed from the circuit and replaced by a short-circuit then the loop becomes a simple LC circuit whose resonance frequency  $f$  is given by (1).

$$2\pi f = \frac{1}{\sqrt{LC}} \quad (1)$$

The proposed methodology to estimate the value of  $f$  and  $L$  consists of measuring the output of the HFCT sensor upon the induction of a fast pulse into the loop. The Fourier spectrum of the recorded signal will show a maximum that corresponds to the value of  $f$ . Finally the value of  $f$  is used in (1) to compute the value of the circuit inductance  $L$ .

The induction of the fast pulse is achieved by using a pulse calibrator that feeds a winding as illustrated in Fig. 3.

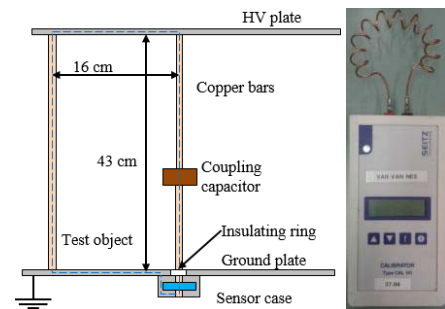


Fig. 3. Induction of a fast pulse into the detection circuit.

For this particular case, the winding has 11 turns arranged in such a way that the magnetic flux enters perpendicular to the plain of the loop. The magnitude of the pulse and the number of turns can be arbitrary chosen as long as the magnitude of the induced pulse is enough to be measured by the HFCT sensor. In fact, if the detection circuit is truly behaving as a simple LC circuit the resonance frequency appears as the main peak in the frequency spectrum. It is worth to mention that for the calculation of the inductance the test object has been short-circuited, see Fig. 3. In this way, the total capacitance of the current loop is the one due to the 2 nF coupling capacitor.

The results of this procedure are shown in Fig. 4. The top graph depicts the signal at the output of the HFCT sensor and the bottom graph corresponds to its frequency spectrum. The frequency corresponding to the maximum peak was 4.7 MHz and therefore after evaluating (1) the inductance of the detection circuit results in 569.3 nH.

### IV. RESONANCE PEAKS IN PD MEASUREMENTS

The inductance of the detection circuit is not expected to change much when the test objects are connected to the set-up.

This is because the compactness of the test cells almost do not modify the geometry and length of the detection circuit. Although the inductance remains almost unchanged, the total capacitance does depend on the series of the coupling capacitor and the test object capacitance. Normally, the coupling capacitance is much bigger than the capacitance of the test object, and since they are connected in series the total capacitance is dominated by the capacitance of the test object. Therefore the circuit resonance frequency has to be evaluated by (1) for each test object.

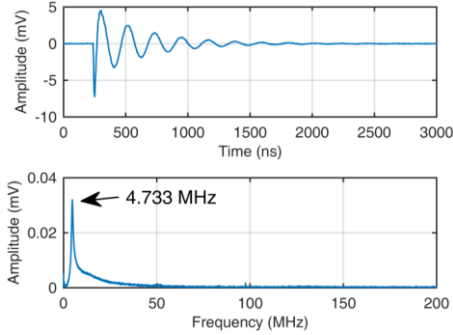


Fig. 4. Induction of a fast pulse into the detection circuit.

In this paper, a number of PD measurements at 6 kV were carried out to validate the frequency characterization methodology described in section III. Three different test cells [8] to produce corona, internal and surface discharges were used whose values of capacitance are summarized in Table 1.

TABLE I. VALUES OF CAPACITANCE AND CIRCUIT RESONANCE FREQUENCY.

$R \approx 0 \Omega L = 569.3 \text{ nH}$		
Type	Capacitance test object	Main Circuit Resonance
Corona	$\sim 1 \text{ pF}$	210.9 MHz
Surface	10 pF	66.7 MHz
Surface	69 pF	25.4 MHz
Internal	89 pF	22.3 MHz

After recording the PD signals at 6 kV, the set-up was de-energized and the response of the detection circuit was measured. Like in the previous section, a pulse was induced into the detection circuit (but this time having the test object connected in the loop) and the output of the HFCT sensor was measured. The results of the measurements are discussed in the following subsections.

### A. Internal Discharges

According to Fig. 5a) the resonance frequency of the detection circuit is around 22.3 MHz which also corresponds to the main frequency peak in the spectrum of any of the measured PD pulses. It is also observed that the amplitude of this frequency is much higher than the other frequency components what suggests the large effect of the LC parameters on the measured PD pulse.

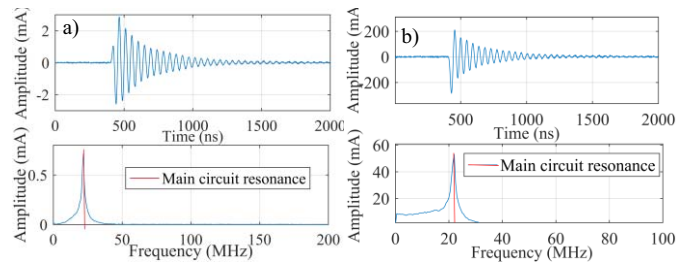


Fig. 5. Frequency response of a) a pulse induced into the detection circuit by a pulse calibrator, b) an actual internal discharge PD pulses.

### B. Surface Discharges

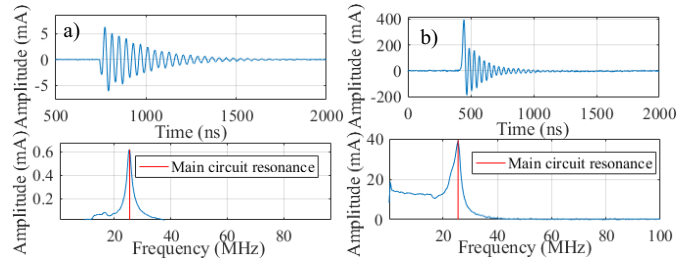


Fig. 6. Frequency response of a) a pulse induced into the detection circuit by a pulse calibrator, b) an actual surface discharge PD pulses. Test object capacitance: 69 pF.

For this surface discharge having a capacitance of 69 pF the resonance frequency was observed at 25.4 MHz, just a bit of an increase compared to the 22.3 MHz obtained for the internal discharges with 89 pF. In order to show the effect of the capacitance, another test cell for surface discharges and 10 pF capacitance was used.

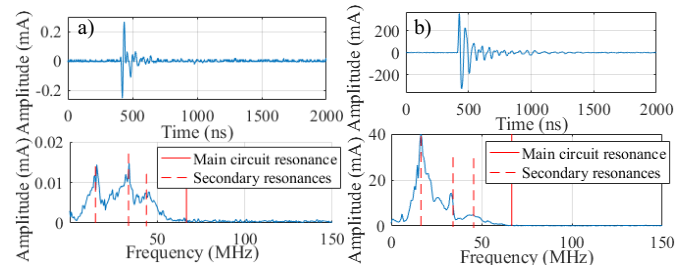


Fig. 7. Frequency response of a) a pulse induced into the detection circuit by a pulse calibrator, b) an actual surface discharge PD pulses. Test object capacitance: 10 pF.

With such a large reduction of the test object capacitance the resonance frequency estimated by (1) is now shifted up to 66.7 MHz. As can be seen, the component at 66.7 MHz is almost not present in the frequency spectrum. However, it is necessary to mention that the bandwidth of the HFCT sensor spans roughly from 35 kHz to 60 MHz meaning that this component may be also attenuated by the sensor. Another important implication of the results in Fig. 7 is that there are additional frequency peaks below 66.7 MHz, observed both in the frequency spectrum of the induced pulse and of the actual PD pulse, that don't correspond to the main LC oscillation of the circuit. Moreover, the shape of the pulse also has changed on account of the several frequency peaks existing in the frequency spectrum.

### C. Corona discharges

When the test cell was replaced by a needle electrode the test object capacitance was reduced to approximately 1 pF and as expected, the resonance frequency estimated by (1) is out of the bandwidth of the sensor. This is an interesting case because it experimentally shows that the resonance frequency of the detection circuit affects strongly the shape and amplitude of the measured PD pulses only when it is located within the bandwidth of the sensor.

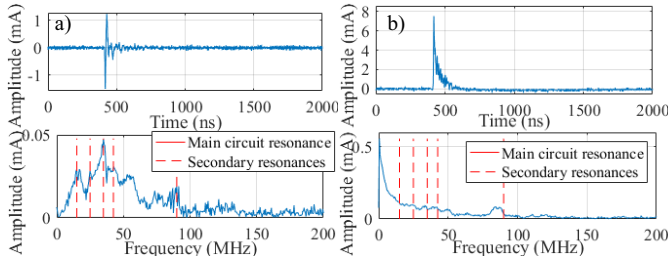


Fig. 8. Frequency response of a) a pulse induced into the detection circuit by a pulse calibrator, b) an actual corona discharge PD pulses. Test object capacitance:  $\sim 1$  pF.

As has been shown, not always the resonance frequency of the detection circuit appears within the bandwidth of the measuring sensor. Its location depends on the LC parameters of the circuit and the capacitance of the test object.

### V. TUNING THE RLC CIRCUIT PARAMETERS

If a given combination of capacitance and inductance is leading to resonance peaks, then this can lead to increase the error in the computation of parameters based on the pulse shape or parameters like charge and energy. The detection circuit affects the measurement results and actions must be taken to reduce it as much as possible. In this work, we have added an extra resistor to the detection circuit in such a way to shift and attenuate the resonance peak by changing its RLC parameters. The value of the resistor that is connected in series with the test object, shown in Fig. 9, is calculated according to (2) and it results in a critically damped response of the detection circuit.

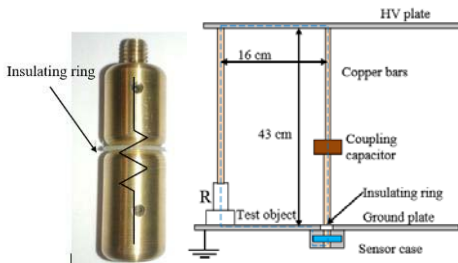


Fig. 9. Connection of the damping resistor in the detection circuit.

$$R_c = 2\sqrt{L/C} \quad (2)$$

For the case of the surface discharge with a test object capacitance of 69 pF the calculated value of the damping resistor was around 180  $\Omega$ . The results show that the resonance peak in Fig. 10a) is not present in Fig. 10b). Therefore all the oscillation brought about by the resonance frequency has disappeared and the PD pulse shape is now almost unipolar.

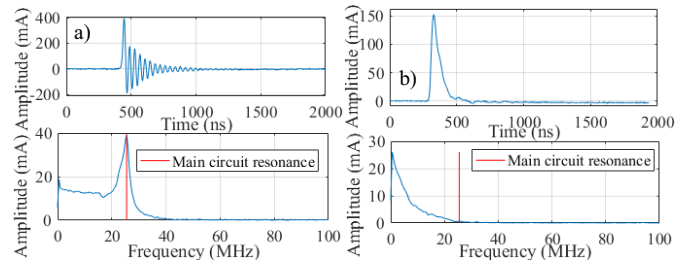


Fig. 10. Effect of damping resistor on the frequency spectrum for a surface discharge PD pulse. Test object capacitance: 69 pF. a) without the damping resistor, b) with damping resistor.

### VI. CONCLUSION

It has been shown that the lengths of the connection cables in a PD measuring set-up may contribute to resonances that distort the amplitude and shape of PD pulse. Long leads and cables are a source of the increase of the ground inductance of the detection circuit and the symmetrical and concentric design of PD set-up described in this paper provides an outstanding way to control the geometry and dimensions and in turn the ground inductances. It was also presented an easy methodology to estimate the equivalent inductance of the set-up, and correspondingly the resonance frequency due to the detection circuit. The possibility to detect resonances due to the set-up itself proved to be useful to recognize the origin of possible oscillations in the recorded PD pulse. Moreover, it was also shown an example of how adding a damping resistor can shift and attenuate resonance peaks out of the bandwidth of the measurement and with this avoid oscillations that may increase the error in the PD-related parameters computation.

### REFERENCES

- [1] A. Rodrigo Mor, L. C. Castro Heredia and F. A. Muñoz, "New clustering techniques based on current peak value, charge and energy calculations for separation of partial discharge sources," IEEE Trans. Dielectr. Electr. Insul., vol. 24, no. 1, pp. 340-348, Feb. 2017.
- [2] A. Rodrigo Mor, L. C. Castro Heredia, and F. A. Muñoz, "Effect of acquisition parameters on equivalent time and equivalent bandwidth algorithms for partial discharge clustering," Int. J. Electr. Power Energy Syst., vol. 88, pp. 141-149, 2017.
- [3] G. Stone, "Importance of bandwidth in PD measurement in operating motors and generators," IEEE Trans. Dielectr. Electr. Insul., vol. 7, no. 1, pp. 6-11, Feb 2000.
- [4] A. Rodrigo Mor, L. C. C. Heredia and F. A. Muñoz, "Estimation of charge, energy and polarity of noisy partial discharge pulses," IEEE Trans. Dielectr. Electr. Insul., vol. 24, no. 4, pp. 2511-2521, 2017.
- [5] S. Boggs, A. Pathak and P. Walker, "Partial discharge. XXII. High frequency attenuation in shielded solid dielectric power cable and implications thereof for PD location," IEEE Electrical Insulation Magazine, vol. 12, no. 1, pp. 9-16, Jan.-Feb. 1996.
- [6] A. Rodrigo Mor, P. H. F. Morshuis and J. J. Smit, "Comparison of charge estimation methods in partial discharge cable measurements," in IEEE Transactions on Dielectrics and Electrical Insulation, vol. 22, no. 2, pp. 657-664, April 2015.
- [7] IEC60270, "High-Voltage Test Techniques –Partial Discharge Measurements", 2000.
- [8] A. Rodrigo Mor, L.C. Castro Heredia, D.A. Harmsen, F.A. Muñoz, "A new design of a test platform for testing multiple partial discharge sources", International Journal of Electrical Power & Energy Systems, vol. 94, pp. 374-384, 2018.